Inorg. Chem. **2002**, *41*, 2505–2517

Charge Transfer of Iron(III) Monomeric and Oligomeric Aqua Hydroxo Complexes: Semiempirical Investigation into Photoactivity

Ludovic Lopes, Joseph de Laat,* and Bernard Legube

Laboratoire de Chimie de l'Eau et de l'Environnement, UMR CNRS 6008, Ecole Supérieure d'Ingénieurs de Poitiers, Université de Poitiers, 40 avenue du Recteur Pineau, 86022 Poitiers Cedex, France

Received October 4, 2001

Aqueous hydrolyses of iron(III) solutions were studied using electronic spectroscopy. Complete spectra from 200 to 800 nm were obtained for the four ferric aqua hydroxo complexes: $Fe(H_2O)_6^{3+}$, $Fe(OH)(H_2O)_5^{2+}$, $Fe(OH)_2(H_2O)_4^{+}$, and the dimer $Fe_2(\mu\text{-}OH)_2(H_2O)_8^{4+}$. Semiempirical Zindo/s calculations were employed to assign which types of electronic transfers are involved so that the photoactivity as regards the photoreduction dissociation $Fe^{III}_{aq} \xrightarrow{h\nu} Fe^{II}_{aq} + OH^{\bullet}$ can be discussed. Fe^{3+} exhibits two LMCT from nonbonding p orbitals (nLp) located at 190 and 240 nm. $Fe(OH)^{2+}$ shows two major $nLp_{OH} \rightarrow d$ transitions at 205 and 295 nm. As regards its geometry, computed investigations using an Fe–OH distance of 2.05 Å better fit than using a shorter distance (~1.8 Å); the same conclusion remains constant for all hydroxo complexes. The dihydroxo form's spectrum was confronted to its common cis and trans expectable isomers plus an unusual pentacoordinate one. Even if the trans isomer is supposed to be the lowest Gibbs free energy species in solution, there is some evidence of the presence of the cis form; hence, both species must be close in energy. Other isolated $nLp_{OH} \rightarrow d$ transfer wavelengths are 235, 245, and 335 nm. As for the dimer, this study provides some clue in favor of the bis(μ-hydroxo)) description. Both water and hydroxo ligands are involved along the electronic transitions toward only d^1 metal-centered orbitals at 220 and 260 nm for H_2O, 335 and 470 nm for OH^-, and 205 nm for both. Charge transfers for the hydrogen oxide bridge form $Fe_2(\mu\text{-}H_3O_2)(H_2O)_8^{5+}$ were also computed. Finally predictions about the two bis(μ-hydroxo) bridge trimer $Fe_3(OH)_4(H_2O)_{10}^{5+}$ enable one to foresee a huge and broad charge transfer in the UV region (~240 nm) followed by a multi $nLp_{OH} \rightarrow d^1$ transfer extending up to ~650 nm.

Introduction

Iron(III) has a strong tendency to hydrolyze in aqueous solution.[1,2] In the pH range below 4 trivalent iron is expected to be present largely in ionic form in solution. In notably acidic media the major monomeric forms are $Fe(H_2O)_6^{3+}$, $Fe(OH)(H_2O)_5^{2+}$, and $Fe(OH)_2(H_2O)_4^{+}$. At low iron(III) concentrations a neutral complex $Fe(OH)_3(H_2O)_3$ can also exist. The dihydroxo species is classically considered through cis and trans isomers. And recently an unexpected dihydroxo form was computed and found to be quite stable, $Fe(OH)_2(H_2O)_3^{+}$, which consists of a pentacoordinated species with an outer-sphere water molecule.[3] At higher pH and/or for higher ionic strengths hydroxo oligomers and polymers appear.[2,4−11] The dimeric form may be present either as an oxo-bridged complex $Fe_2(\mu\text{-}O)(H_2O)_8^{4+}$ or as a dihydroxo-bridged one $Fe_2(\mu\text{-}OH)_2(H_2O)_8^{4+}$; they may be close in energy.[2] There is still some discrepancy[12] between these two

* To whom correspondence should be addressed. E-mail: joseph.delaat@esip.univ-poitiers.fr.

(1) Sylva, R. N. *Rev. Pure Appl. Chem.* **1972**, *22*, 115−132.
(2) Flynn, C. M. *Chem. Rev.* **1984**, *84*, 31−41.
(3) Martin, R. L.; Hay, P. J.; Pratt, L. R. *J. Phys. Chem. A* **1998**, *102*, 3565−3573.
(4) Rabinowitch, E.; Stockmayer, W. H. *J. Am. Chem. Soc.* **1942**, *64*, 4, 335−347.
(5) Milburn, R. M.; Vosburgh, W. C. *J. Am. Chem. Soc.* **1955**, *77*, 1352−1355.
(6) Milburn, R. M. *J. Am. Chem. Soc.* **1957**, *79*, 537−540.
(7) Knight, R. J.; Sylva, R. N. *J. Inorg. Nucl. Chem.* **1974**, *36*, 591−597.
(8) Mulay, L. N.; Selwood, P. W. *J. Am. Chem. Soc.* **1954**, *77*, 2693−2697.
(9) Spiro, T. G.; Allerton, S. E.; Renner, J.; Terzis, A.; Bils, R.; Saltman, P. *J. Am. Chem. Soc.* **1966**, *88*, 2721−2726.
(10) Allerton, S. E.; Remer, J.; Colts, S.; Saltman, P. *J. Am. Chem. Soc.* **1966**, *88*, 3147−3148.
(11) Danesi, P. R.; Chiarizia, R.; Scibona, G.; Riccardi, R. *Inorg. Chem.* **1973**, *12*, 2089−2091.
(12) Knudsen, J. M.; Larsen, E.; Moreira, J. E.; Nielsen, O. F. *Acta Chem. Scand. A* **1975**, *25*, 833−839.

10.1021/ic011029m CCC: $22.00
Published on Web 04/11/2002

forms; however, the dihydroxo-bridged notation is more commonly met in the literature.[8,12−15] A monohydroxo dimer $Fe_2(\mu\text{-}OH)(H_2O)_8^{5+}$ was proposed once[16] and revisited using Mössbauer spectroscopy, which finally submitted a proposal for another dimeric form with a hydrogen oxide bridge $Fe_2(\mu\text{-}H_3O_2)(H_2O)_8^{5+}$ instead.[17−19] A trimeric complex was also considered both as a linear form[15,20,21] $Fe_3(\mu\text{-}OH)_4(H_2O)_{10}^{5+}$ with two hydroxo bridges and as a cyclic form[14] $Fe_3(\mu\text{-}OH)_3(H_2O)_{10}^{6+}$, where each ferric ion is linked to the others via a single hydroxo ligand. A longer polymer such as $Fe_{12}(OH)_{34}^{2+}$ was also proposed[22] and refuted afterward;[23] however, an equilibrium formation constant was published quite recently.[24]

As regards ferric aqueous hydroxo monomers, they feature spectra overlapping partly solar radiation (wavelengths above 290 nm),[25−31] and high-concentration iron(III) solutions are well-known for being strongly red colored.[2,4−7] Ferric hydroxo complexes are famous for undergoing photoreduction[28,32−41] that generates the $OH^\bullet$ radical. The general pattern of this photolysis is

$$Fe^{III}_{aq} \xrightarrow{h\nu} Fe^{II}_{aq} + OH^\bullet$$

This photoactivity is generally attributed to ligand to metal charge transfers (LMCT) involving nonbonding p-orbitals centered on the OH^- ligands (nLp_{OH}).[34] However there is still no complete study of charge-transfer bands of iron(III) aqueous species. Given that aqueous ferric ions are present in surface water and are mainly soluble in more acidic environment of atmospheric droplets, these complexes are potential photolytic sources of $OH^\bullet$ radicals in natural media. This photochemical step was also shown to be important during Fe^{3+}/Fe^{2+} recycling in marine waters.[42] Recently the $Fe(OH)^{2+}$ species was considered to account for enhancement of Fenton processes (catalytic decomposition of hydrogen peroxyde by Fe^{II} salts) through photoassistance.[43−45]

The aim of this work is to study the hydrolysis of aqueous iron(III) using electronic spectroscopy to reach the complete spectrum from the UV region to infrared (200−800 nm) for each major aqua hydroxo complex so that intrinsic potential photoactivity of each species will be reached. Subsequently, these results will be confronted with calculations from the Zindo/s semiempirical method which was used to estimate the energy levels of the molecular orbitals of all complexes. So main bands for each obtained spectrum will be interpreted. In addition some elements concerning iron(III) inorganic chemistry will be presented.

Experimental Section

Reagents and Solutions. $Fe(ClO_4)_3{\cdot}nH_2O$ (Aldrich, low chloride), $HClO_4$ (Riedel-de Haën, ACS reagent), $NaClO_4$ (Sigma), and NaOH (Labosi, Analynorm, 1 M) were used as received. All aqueous solutions were made up with Milli-Q water. Since iron(III) perchlorate has a great tendency to hydrate, its degree of hydration (i.e. its effective molecular weight) was checked regularly by spectrophotometric titration using 1,10-*o*-phenanthroline.[46] Aliquots of Fe(III) solutions were reduced to Fe(II) with hydroxylammonium chloride, and then the concentration of Fe(II) formed was measured (pH $\sim$ 4.5/λ = 510 nm). The molar extinction coefficient of $Fe(ophen)_3^{2+}$ was found to be ϵ_{510} = 10 950 L·mol^{-1}·cm^{-1}. Solutions of Fe(III) were prepared by dissolving the required amount of iron(III) perchlorate in water acidified with $HClO_4$ and containing $NaClO_4$ needed to fix the ionic strength. $HClO_4$ quantities were adjustable, depending on the desired pH. When higher pH values were requested, sodium hydroxide aliquots were used to adjust them. At low pH (<3) and for an ionic strength of I = 0.1 mol·L^{-1}, the pH and electronic spectrum of iron(III) solutions were stable for several days. At pH between 3.5 and 4 using I = 1 mol·L^{-1}, all iron(III) solutions were freshly prepared each time before use to limit potential maturation toward metastable long-chain polymers; spectroscopic measurements were carried out just after preparation. Moreover, even for I = 1 mol·L^{-1}, total iron(III) concentration stayed below 1 mmol·L^{-1}, which is rather low compared to previous studies[21] involving up to $\sim$20 mmol·L^{-1}. Anyway, pH or absorbance measurements with iron(III) solutions are known to be delicate.[2,47]

Instrumentation. pH measurements were conducted using a pHm 240 (Tacussel), calibrated with five buffers: pH = 1.09/1.68/4.005 (Radiometer Analytical) and 2.00/3.00 (Labosi). All the spectra were recorded on a SAFAS 190 DES spectrophotometer.

(13) Schugar, H.; Walling, C.; Jones, R. B.; Gray, H. B. *J. Am. Chem. Soc.* **1967**, *89*, 3712−3720.
(14) Sommer, B. A.; Margerum, D. W. *Inorg. Chem.* **1970**, *9*, 2517−2521.
(15) Lente, G.; Fábián, I. *Inorg. Chem.* **1999**, *38*, 603−605.
(16) Ropars, C.; Rougée, M.; Momenteau, M.; Lexa, D. *J. Chim. Phys. Phys.-Chim. Biol.* **1968**, *65*, 816−822.
(17) Pan, H. K.; Yarusso, D. J.; Knapp, G. S.; Pineri, M.; Meagher, A.; Coey, J. M. D.; Cooper, S. L. *J. Chem. Phys.* **1983**, *79*, 4736−4745.
(18) Meagher, A. *Inorg. Chim. Acta* **1988**, *146*, 19−23.
(19) Meagher, A.; Rodmacq, B. *New J. Chem.* **1988**, *12*, 961−964.
(20) Arnek, R.; Schylter, K. *Acta Chem. Scand.* **1968**, *22*, 1327.
(21) Khoe, G. H.; Brown, P. L.; Sylva, R. N.; Robins R. G. *J. Chem. Soc., Dalton. Trans.* **1986**, 1901−1906.
(22) Ciavatta, L.; Grimaldi, M. *J. Inorg. Nucl. Chem.* **1975**, *37*, 163.
(23) Dousma, J.; De Bruyn, P. L. *J. Colloid Interface Sci.* **1976**, *56*, 527.
(24) Daniele, P. G.; Rigano, G.; Sammartano, S.; Zelano, V. *Talanta* **1994**, *41*, 1577−1582.
(25) Turner, R. C.; Miles, K. E. *Can. J. Chem.* **1957**, *35*, 1002−1009.
(26) Escot, M. T. Ph.D. Thesis, University of Clermont-Ferrand, Clermont-Ferrand, France, 1973.
(27) Knight, R. J.; Sylva, R. N. *J. Inorg. Nucl. Chem.* **1975**, *37*, 779−783.
(28) Benkelberg, H. J.; Warneck, P. *J. Phys. Chem.* **1995**, *99*, 5214−5221.
(29) Woods, M. J. M. *Studies of Complex Ion Equilibria I. Iron(III) Chloride System II. Thallium(III) Chloride System*; University Microfilm Inc.: Ann Arbor, MI, 1961.
(30) Byrne, R. H.; Kester, D. R. *J. Solution Chem.* **1981**, *10*, 51−67.
(31) Jacobsen, F.; Holcman, J.; Sehested, K. *Int. J. Chem. Kinet.* **1997**, *29*, 17−24.
(32) Evans, M. G.; Uri, N. *Nature* **1949**, *164*, 404−405.
(33) Evans, M. G.; Santappa, M.; Uri, N. *J. Polym. Sci.* **1951**, *7*, 243−260.
(34) David, F.; David, P. G. *J. Phys. Chem.* **1976**, *80*, 579−583.
(35) Baxendale, J. H.; Magee, J. *Trans. Faraday. Soc.* **1955**, *51*, 205−213.
(36) Faust, B. C.; Hoigné, J. *Atmos. Environ.* **1990**, *24A*, 79−89.
(37) Langford, C. H.; Carey, J. H. *Can. J. Chem.* **1975**, *53*, 2430−2435.
(38) Carey, J. H.; Langford, C. H. *Can. J. Chem.* **1975**, *53*, 2436−2440.
(39) Buxton, G.V.; Wilford, S. P.; Williams, R. J. *J. Chem. Soc.* **1962**, 4957−4962.
(40) Kawaguchi, H.; Inagaki, A. *Chemosphere* **1993**, *27*, 2381−2387.
(41) Feng, W.; Nansheng, D. *Chemosphere* **2000**, *41*, 1137−1147.
(42) Byrne, R. H.; Kester, D. R. *J. Solution Chem.* **1978**, *7*, 373−383.
(43) Ruppert, G.; Bauer, G.; Heisler, G. *J. Photochem. Photobiol., A* **1993**, *73*, 75.
(44) Lipchynska-Kochany, E. *Environ. Sci. Technol.* **1992**, *26*, 313.
(45) Pignatello, J. *Environ. Sci. Technol.* **1992**, *26*, 944.
(46) *Eaux, Méthodes d'essai-Recueil de Normes Françaises*, 4th ed.; AFNOR: Paris, 1990.
(47) Nadtochenko, V. A.; Kiwi, J. *Inorg. Chem.* **1998**, *37*, 5233−5238.

Table 1. Equilibrium Constants and Enthalpies of Reaction for Iron(III) Hydrolysis

K_{ij}	log K_{ij}	ref	$\Delta_r H°$ ($kJ·mol^{-1}$)	ref
K_{11}	$-2.17 - 2.04I^{1/2}/(I + 2.4I^{1/2}) - 0.01I$	5	43.5	50
K_{12}	$-5.67 - 3.066I^{1/2}/(I + 3.71I^{1/2}) - 0.16I$	48	64.2	50
K_{13}	$-12 - 3.066I^{1/2}/(I + 3.81\,I^{1/2}) - 0.07I$	48		
K_{22}	-2.9	49	41.7	50
K_{21}[a]	-0.98	16		
K_{34}[b]	-6.98	21		
K_{13s}	-37.1	2		

[a] Constant determined for $I = 0.1$ mol.L^{-1} ($NaClO_4$) and linked to $Fe_2(\mu\text{-}OH)^{5+}$ by ref 16 and afterward to $Fe_2(\mu\text{-}H_3O_2)^{5+}$ by ref 18. [b] Quite recent value computed for $I = 1$ mol·L^{-1} in a very poorly complexing medium (KNO_3).[21]

Results and Discussion

Equilibria. In acidic solutions of iron(III), the speciation is governed by the following equilibria:

$$Fe^{3+}_{aq} \rightleftarrows Fe(OH)^{2+} + H^+_{aq} \quad K_{11}$$

$$Fe^{3+}_{aq} \rightleftarrows Fe(OH)_2{}^{+} + 2H^+_{aq} \quad K_{12}$$

$$Fe^{3+}_{aq} \rightleftarrows Fe(OH)_3 + 3H^+_{aq} \quad K_{13}$$

$$2Fe^{3+}_{aq} \rightleftarrows Fe_2(OH)_2{}^{4+} + 2H^+_{aq} + 2H_2O \quad K_{22}$$

$$2Fe^{3+}_{aq} \rightleftarrows Fe_2(H_3O_2)^{5+} + H^+_{aq} \quad K_{21}$$

$$3Fe^{3+}_{aq} \rightleftarrows Fe_3(OH)_4{}^{5+} + 4H^+_{aq} + 4H_2O \quad K_{34}$$

$$12Fe^{3+}_{aq} \rightleftarrows Fe_{12}(OH)_{34}{}^{2+} + 34H^+_{aq} + 22H_2O \quad K_{12/34}$$

$$Fe(OH)_3(s) \rightleftarrows Fe^{3+}_{aq} + 3OH^- \quad K_{13s}$$

Values for the equilibrium constants and enthalpies of reaction at $T = 298$ K are given in Table 1, followed by ionic strength corrections that were previously proposed.

Potential complexation between iron(III) and the counteranion ClO_4^- also has to be mentioned:

$$Fe^{3+}_{aq} + n ClO_4{}^- \rightleftarrows Fe(ClO_4)_n^{(3-n)+} + nH_2O$$

Previous studies were led using perchlorate concentrations up to 3 mol·L^{-1} without any sign of complexation.[4] However some authors have proposed weak values for the first association constant:[51] $10^{1.15}$ ($I = 0$ M; 25 °C);[52] $10^{1.28}$ (19 °C);[53] $10^{0.26}$ ($I = 0$ M, 20 °C);[54] $10^{0.30}$ ($I = 0$ M, 25 °C).[24] Other papers refute this hypothesis,[55] and commonly this reaction of complexation is not considered.[42,56]

The value of K_{12} that is used here is the value computed by Turner et al.[48] Recent surveys concluded that the hydrolysis constants that can be found in the literature are controversial.[57,58] Finally the review of Byrne et al.[57] shows that a variety of recent works have indicated that, at 25 °C and 0.7 M ionic strength, log K_{12} is smaller than or approximately equal to -7, which corresponds to log $K_{12} = -6.08$ s at $I = 0$ M, using Davies' equation to correct the constant from 0.7 to 0 M. This value is quite close to log $K_{12} = -5.67$ presented in Table 1. On the other hand, another very recent determination gave a higher value.[58] On this basis, we kept and employed thereafter the constant determined by Turner et al.[48]

About the hydrogen oxide bridged dimer, $Fe_2(H_3O_2)^{5+}$ has only been observed for quite concentrated solutions[18,19] ($[Fe^{III}]_{tot}$ up to 0.2 mol·L^{-1}) in Nafion membranes. The membrane matrix is generally supposed to have no influence on the cations in the aqueous phase, and therefore, those systems are considered to give relevant conclusions for high concentration solutions. These types of complexes are more commonly observed in clusters or crystals than in solutions.[59] Considering that the solutions studied here were far less concentrated ($[Fe^{III}]_{tot}$ remained below 1 mmol·L^{-1}), this species is discarded, assuming that it is not substantially formed under the present experimental conditions. As regards the hydrolysis constant[16] K_{21} presented in Table 1, previous recomputations[21] of the hydrolysis constants did not succeed in fitting models containing the (2,1) stoichiometry on the basis of experiments in perchlorate, nitrate, or chloride media, using $I = 1$ mol·L^{-1} and total iron(III) concentrations between ~0.2 and ~20 mM. So this constant may be overestimated. As for long-chain polymers (for instance the possible $Fe_{12}(OH)_{34}{}^{2+}$), they must not be obtained here because of the "rather low" total iron(III) concentrations. Hence, the final set of aqua hydroxo complexes kept through this work consists of the (1,0), (1,1), (1,2), (1,3), (2,2), and (3,4) stoichiometries.

Spectrophotometry Results at *I* = *0.1 M*. This study was carried out at 18 °C, and the pH values of the iron(III) solutions were between 1.07 and 3.05, with constant ionic strength $I = 0.1$ M adjusted using $NaClO_4$. This has been completed by two additional spectra for $[HClO_4] = 0.5$ and 1 mol·L^{-1}. Two isosbestic points at wavelengths of 225 nm ($\epsilon \sim 3550$ L·mol^{-1}·cm^{-1}) and 272 nm ($\epsilon \sim 1475$ L·mol^{-1}·cm^{-1}) are noted on the set of recorded absorption spectra. Both isosbestic points have already been reported[5,28,60] at the same wavelengths 224−225 and 272−274 nm.

Iron(III) ionic distribution depends on the pH of the solution and on the total iron concentration. Speciation calculations were made after correcting the effective equilibrium constants for $T = 18$ °C (van't Hoff law) and $I =$

(48) Turner, D. R.; Whitfield, M.; Dickson, A. G. *Geochim. Cosmochim. Acta* **1981**, *45*, 855−881.
(49) Baes, C. F.; Mesmer, R. E. *The Hydrolysis of Cations*; Wiley: New York, 1976.
(50) Martell, A. M.; Smith, R. M. *Critical Stability Constants*; Plenum: New York, 1977; Vol. 3.
(51) Stipp, S. L. *Environ. Sci. Technol.* **1990**, *24*, 699−705.
(52) Martell, A. M.; Smith, R. M. *Critical Stability Constants*; Plenum: New York, 1976.
(53) Sykes, K. W. *Spec. Publ. Chem. Soc.* **1954**, *1*, 64−74.
(54) Fordham A. W. *Aust. J. Chem.* **1969**, *22*, 1111−1122.
(55) Richards, D. H.; Sykes, K. W. *J. Chem. Soc.* **1960**, 3626−3633.
(56) Sapieszko, R. S.; Patel, R. C.; Matijevic, E. *J. Phys. Chem.* **1977**, *81*, 1061−1068.
(57) Byrne, R. H.; Luo, Y.-R.; Young, R. W. *Mar. Chem.* **2000**, *70*, 23−35.
(58) Millero, F. J.; Wensheng, Y.; Aicher, J. *Mar. Chem.* **1995**, *50*, 21−39.
(59) Bino, A.; Gibson, D. *J. Am. Chem. Soc.* **1982**, *104*, 4383−4388.
(60) Olson, A. R.; Simonson, T. R.; *J. Chem. Phys.* **1949**, *17*, 1322−1325.

0.1 mol·L^{-1} using extended Debye−Hückel or Davies corrections for activity coefficients (γ). Since the highest iron(III) concentration used here was 548 μmol·L^{-1} and the pH remains below 3.05, the speciation is essentially governed by Fe^{3+}_{aq} and $Fe(OH)^{2+}$. If $[HClO_4] = h_0$ and y is the amount of H^+ generated by iron(III) first hydrolysis, y is the positive solution of the equation

$$y^2 + y(h_0 + K_{11}) - K_{11}C = 0$$

where C refers to iron(III) total concentration; thus, pH = $-\log[\gamma_{H^+}(h_0 + y)]$. So in this part the pH values were calculated from h_0 and C and the pH values given here are calculated ones. They were very close to experimental pH values that were checked (standard deviation: ±0.05 pH unit).

Summing the absorbance of Fe^{3+}_{aq} and $Fe(OH)^{2+}$ for the most acidic solutions gives

$$\epsilon = \epsilon_1 f/C + \epsilon_2 K_{11} f/hC \quad (1)$$

where ϵ_1 refers to Fe^{3+}_{aq}, ϵ_2 to $Fe(OH)^{2+}$, $[H^+_{aq}]$ is called h, and $[Fe^{3+}_{aq}] = f$. When $1/h \rightarrow 0$, then $f/C \rightarrow 1$, and this ratio can be developed using a second-order expression

$$f/C \sim 1 + \alpha_1/h + \alpha_2/h^2 \quad (2)$$

Moreover for very highly acidic media, the ionic strength $I \sim h$ varies, which entails a deviation for K_{11} from its value for $I = H = 0.1$ mol·L^{-1}. Therefore, this equilibrium constant can be developed via a second-order expression:

$$K_{11} \sim K' + \beta_1(1/h - 1/H) + \beta_2(1/h - 1/H)^2 \quad (3)$$

Then (1)−(3) lead to

$$\epsilon \sim \epsilon_1 + \delta_1/h + \delta_2/h^2$$

where δ_1 and δ_2 are functions of ϵ_1, ϵ_2, α_1, α_2, K', H, β_1, and β_2. Then plotting ϵ versus $1/h$ for each wavelength and fitting using a second-order polynomial results in the y-axis intercept yielding ϵ_1. Some graphical extrapolations of effective absorption coefficients measured at various pH values low enough to make Fe^{3+}_{aq} and $Fe(OH)^{2+}$ be the major species in solution were previously used.[5] Electronic spectra of Fe^{3+}_{aq} agree well with other published results from Turner et al.,[25] Escot,[26] Knight and Sylva,[27] Benkelberg and Warneck,[28] Woods[29] (values treated by Byrne at al), and Byrne and Kester[30] (data from the last three groups were taken from published tables). Its spectrum exhibits two main absorption bands, the first one at $\lambda \sim 240$ nm and the second one centered a little bit below 200 nm.

By writing

$$\epsilon = (\epsilon_1 + \epsilon_2 K_{11}/h)/(1 + K_{11}/h)$$

through this set of data, it was also possible to recheck the value of K_{11}. One procedure[55] uses the following equation:

$$(h_0 - h)/(\epsilon - \epsilon_0) = (K_{11} + h)(K_{11} + h_0)/(K_{11}(\epsilon_2 - \epsilon_1))$$

Here h_0 refers to a fixed hydrogen ion concentration solution and ϵ_0 is its extinction coefficient. Therefore, a plot of $(h_0 - h)/(\epsilon - \epsilon_0)$ versus h should yield a straight line leading to K_{11} as the ratio of y-axis intercept to slope. This method was applied to wavelengths from 200 to 360 nm every 5 nm ; the reference pH was 1.78, and the pH values of the media that were considered were between 2.07 and 3.05. Data close to the isosbestic points were discarded because in these regions ϵ_1 and ϵ_2 are quite similar, and within their respective uncertainties, the difference $\epsilon_2 - \epsilon_1$ can entail divergences. This led to 24 determinations of K_{11} whose average value at the temperature and the ionic strength employed is $K_{11} = 1.93 \times 10^{-3}$ mol·L^{-1}. Correction to $T =$ 25 °C and $I = 0$ mol·L^{-1} using the reaction enthalpy and the Debye−Hückel type equation given in Table 1 finally yields $-\log K_{11} = 2.16$ ($T = 25$ °C, $I = 0$ M). This value is consistent with a review on aqueous iron(III) solutions that gives $-\log K_{11} \sim 2.2$ (±0.1−0.2);[2] in addition other recent redeterminations[28,57] yielded $-\log K_{11} = 2.17-2.18$.

As regards ϵ_2, this extinction coefficient is determined using K_{11} (used to calculate molar fractions), and published results usually consist in average values found for several pH values.[25,27,28] When x_1 and x_2 are defined as the respective molar fractions of Fe^{3+}_{aq} and $Fe(OH)^{2+}$

$$\epsilon = \epsilon_1 x_1 + \epsilon_2 x_2$$

Thus,

$$\epsilon - \epsilon_1 x_1 = \epsilon_2(1 - x_1)$$

Hence, since ϵ_1 was previously extrapolated, plotting $\epsilon - \epsilon_1 x_1$ versus x_1 gives a double determination of ϵ_2 at the same time through the slope and the y-axis intercept, by using the whole set of collected data. The consistence between the two values calculated (via the slope and the axis intercept) through this double determination method was good for all wavelengths. The agreement between this work and different previously determined spectra from Escot,[26] Knight and Sylva,[27] Benkelberg and Warneck,[28] Faust and Hoigné,[36] and Byrne and Kester[30] (data from the last three groups were taken from published tables) is good. For this species the major electronic transitions are located at wavelengths $\lambda \sim$ 205 nm and $\lambda \sim 295$ nm.

Spectrophotometry Results at $I = 1$ mol·L^{-1}. To get the electronic spectra of $Fe(OH)_2^+$ and $Fe_2(OH)_2^{4+}$ higher pH values and iron(III) total concentration have to be reached. Therefore noteworthy molar fractions of these two aqua hydroxo complexes are obtained. In addition there are some doubts about the K_{13} value,[58] which is sometimes considered as being overevaluated. In this section absorbances of ferric solutions ($[Fe^{III}]_{tot} \sim 900$ μmol·L^{-1}) with high ionic strength ($I = 1$ mol·L^{-1}) have been recorded at 25 °C. The pH values of these media were between 3.57 and 4.03 and was adjusted by adding small amounts of NaOH (1 M) to large volumes of iron(III) perchlorate solutions. Considering the pH values all these solutions were close to the saturation cutoff, no precipitation was observed. However, this saturation limit is calculated via K_{13s}, whose value

is given with some uncertainty,[2] and one can expect potential oversaturated solutions to need time to evolve toward precipitation. The speciation was calculated using a previously determined ionic strength correction for K_{11} and K_{12} (see Table 1) and the Davies' equation for correcting activity coefficients. If label 3 refers to $Fe(OH)_2^{+}$ and 4 to $Fe_2(OH)_2^{4+}$, then the ranges of the molar fractions were from $x_3 = 0.111$ to 0.301 as for the dihydroxo complex and from $x_4 = 0.113$ to 0.133 as regards the dimer. The molar fraction for the trimeric form was always very low (<0.4% for the highest one); thus, this species was discarded. Under these conditions

$$\epsilon = \epsilon_1 x_1 + \epsilon_2 x_2 + \epsilon_3 x_3 + \epsilon_4 x_4$$

Then

$$(\epsilon - \epsilon_1 x_1 - \epsilon_2 x_2)/x_4 = \epsilon_3 x_3/x_4 + \epsilon_4$$

and

$$(\epsilon - \epsilon_1 x_1 - \epsilon_2 x_2)/x_3 = \epsilon_3 + \epsilon_4 x_4/x_3$$

Since ϵ_1 and ϵ_2 have been determined, then these two equations can lead to ϵ_3 and ϵ_4 by plotting $(\epsilon - \epsilon_1 x_1 - \epsilon_2 x_2)/x_4$ versus x_3/x_4 and $(\epsilon - \epsilon_1 x_1 - \epsilon_2 x_2)/x_3$ versus x_4/x_3. Each linear fit should give determinations of both ϵ_3 and ϵ_4 values using the slopes and the *y*-axis intercepts. This way, exploiting the same set of data allows the spectra of $Fe(OH)_2^{+}$ and $Fe_2(OH)_2^{4+}$ to be calculated twice. For all wavelengths there is a good and consistent agreement between the values determined using the slope of the fitting straight line and the axis intercept: the standard deviation between the two methods is up to ±7% for the dimeric form (considering the 200−500 nm range) and up to 15% for the monomeric one. All the graphic extrapolations gave good straight lines indicating that there was no obvious sign for any precipitation or change in the set of the present species in solution. Several series of pH values and total iron(III) concentrations have been used, then the electronic spectra of $Fe(OH)_2^{+}$ and $Fe_2(OH)_2^{4+}$ were determined by calculating the average of all results given by all series and for each one by the two methods (extrapolations using the slope or the *y*-axis intercept). Some discrepancies exist between the spectra obtained here and other studies. Concerning $Fe(OH)_2^{+}$, there are few results on this species[26,27] and generally its absorption spectra are considered to be very close to that of $Fe(OH)^{2+}$ with a major absorption band centered around $\lambda \sim 300$ nm.[28] Discrepancies are probably due to differences in the hydrolysis constants that are employed to reach the solutions' composition. For instance Knight and Sylva[27] did not succeed in determining K_{12} and the spectrum of $Fe(OH)_2^{+}$ they obtained is based on the rough estimate $K_{12} \sim 10^{-7}$ taken from Hedstrom's work[61] (1953) for ionic strength $I = 0.1$ M. This value corresponds to log $K_{12} = -6.31$ ($I = 0$ M), which is clearly below the proposed cutoff value of log $K_{12} \sim -5.89$ that can be derived from the recent survey of Byrne et al.[57] using Davies' correction. Here two peaks were found for short wavelengths $\lambda \sim 210$ nm and $\lambda \sim 245$ nm, while results of Knight and Sylva show no maximum in this region.[27] The shortest energy transition is located around $\lambda \sim 335$ nm. As regards the iron(III) dimer, its electronic spectrum exhibits several bands with shoulders as was previously described.[27] The absorption band centered at $\lambda \sim 335$ nm found here is constant through the whole set of spectra that have been published; however, there are large discrepancies[26,27,31] between the value of the molar extinction coefficient for this wavelength, from 3200 to 9990 $L \cdot mol^{-1} \cdot cm^{-1}$ for the present work. The value found here is much higher than others, but such a high value was already presented ($\epsilon_4^{335\ nm} \sim 8300$ $L \cdot mol^{-1} \cdot cm^{-1}$).[37] This complex has very strong absorption coefficients in the UV region between 200 and 300 nm, and some authors have already given high values for this species ($\epsilon_4^{240\ nm} \sim 12000$ $L \cdot mol^{-1} \cdot cm^{-1}$).[27] Here again, there are few previous studies to make comparisons with and the differences are mostly tied to thermodynamic constant speciation calculations. Considering the data from Jacobsen et al.,[31] the envelope of the graph they published is rather close to that obtained here except that a clear offset exists between the given extinction coefficients. But it has to be mentioned that their spectra were normalized to $\epsilon_4^{335\ nm} = 3200$ $L \cdot mol^{-1} \cdot cm^{-1}$ and unfortunately the value that was obtained before correcting the offset was not presented. To conclude on this species, this dimeric form has a tale extending into the visible radiation region, which is consistent with the intense red-brown color of high iron(III) concentration solutions, generally attributed to the dimer and further oligomeric or polymeric forms.[2,4−7]

Computational Details. The semiempirical calculations in this study have been carried out using the Hyperchem 5.1 program package.[62] The ZINDO/S method[63−65] parametrized to reproduce UV−visible electronic transitions has been used to estimate the molecular orbitals diagrams of the iron(III) aqua hydroxo complexes. This method has been previously used to reproduce spectra of several complexes and more particularly for studying the spectroscopy of internal d−d excitations of hydrated ions of the first transition-metal series.[64] RHF spin pairing has been selected in addition the standard SCF controls (with accelerated convergence), and overlap weighting factors have been kept.

First and separately the aqueous ligands H_2O and OH^- have been optimized using the same set of parameters. This geometrical computation led to $d_{OH} = 0.99$ Å and HOH = 100° for H_2O and $d_{OH} = 1.05$ Å for OH^-. These results have been applied for both ligands in each calculation thereafter. Then several complexes have been considered and computed, first the monomeric forms, $Fe(H_2O)_6^{3+}$, $Fe(OH)(H_2O)_5^{2+}$, $Fe(OH)_2(H_2O)_4^{+}$ cis and trans isomers, and $Fe(OH)_2(H_2O)_3^{+}$, where one coordinating water molecule is removed out of the first hydration shell. Some oligomers were also studied:

(61) Hedström, B. O. A. *Ark. Kemi* **1953**, *6*, 1−16.
(62) *Hyperchem 5.1*; Hypercube Inc.: 1996.
(63) Bacon, A. D.; Zerner, M. C. *Theor. Chim. Acta* **1979**, *53*, 21.
(64) Anderson; Edwards; Zerner, M. C. *Inorg. Chem.* **1986**, *25*, 2728−2732.
(65) Ridley, J. E.; Zerner, M. C. *Theor. Chim. Acta* **1976**, *42*, 223.

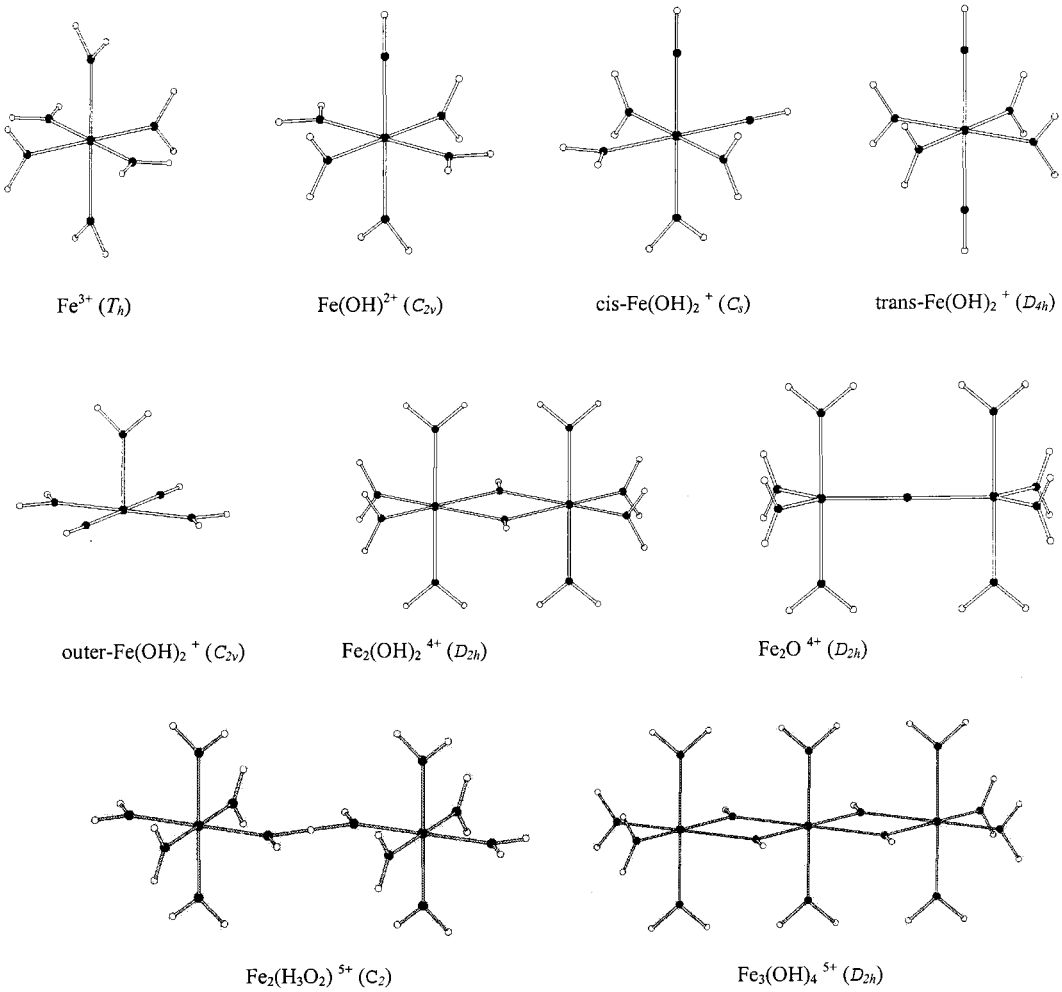

Figure 1. Computed structures of the studied aqua hydroxo complexes and their single point group.

the bis(μ-hydroxo) dimer $Fe_2(OH)_2(H_2O)_8^{4+}$, the μ-oxo one $Fe_2O(H_2O)_8^{4+}$, and the linear bis(μ-hydroxo) trimeric species $Fe_3(OH)_4(H_2O)_{10}^{5+}$. The speculated hydrogen oxide dimer $Fe_2(\mu\text{-}H_3O_2)(H_2O)_{10}^{5+}$ was also investigated. For this computation the internal hydrogen bond O---H---O was considered to lead to an oxygen to oxygen distance of 2.5 Å, meaning $d_{O-H(-O)} = 1.25$ Å, with a linear O−H−O pattern according to previous works on this ligand.[59,66,67] The other d_{O-H} distance was kept equal to 0.99 Å, and the angle HOH, to 100°. Usually ferric aqueous ions are described with an octahedral geometry. However $Fe(OH)_4^-$ was recently presented in tetrahedral coordination[68] in contrast with previous predictions.[69] For each aqua hydroxo complex the chosen core geometry of each ferric ion is octahedral, except for the μ-oxo dimer, where the linear pattern Fe−O−Fe was chosen to be associated to a trigonal bipyramid as regards the iron(III) environment. All monomeric structures were built from a T_h conformation for the hexaaqua ion, which is generally considered as the optimal geometry compromise between electrostatic interactions and steric strain between ligands.[3,68,70−72] Figure 1 presents the computed structures and their single point groups. For this first approach all the hydration shell water molecules are considered to be planarly ligating. Due to the octahedral geometry and given that the distance between two ferric ions in polymeric species was experimentally found[73] to be near 3.5 Å, in oligomeric bis(μ-hydroxo) forms the distance $d_{Fe-O(H)} = 2.47$ Å was chosen. Considering that the oxygen atoms in H_2O, OH^-, and O^{2-} have the same ionic radii (1.40−1.45 Å), the bond length between Fe^{3+} and O^{2-} in the μ-oxo species was set to be 2.05 Å. However, two panels of data can be used: those from experimental measurements (EXAFS, neutron scattering, crystallographic determinations) or computed ones. Generally in X-ray experiments on hydroxo-containing polymers, the radii of all the oxygen ligands are considered to be equal,[70,73] and using a value of 0.60−0.64 Å for the radii of Fe^{3+} leads to a nearly constant Fe−O distance of 2.05 Å. The range of distances that were experimentally determined is 1.97−2.05 Å for the hexaaqua ion;[24,70,73−78]

(66) Bino, A.; Gibson, D. *J. Am. Chem. Soc.* **1981**, *103*, 3, 6741−6742.
(67) Bino, A.; Gibson, D. *Inorg. Chem.* **1984**, *23*, 109−115.
(68) Kubicki, J. D. *J. Phys. Chem. A* **2001**, *105*, 8756−8762.
(69) Martin, R. B. *J. Inorg. Biochem* **1991**, *44*, 141.
(70) Caminti, R.; Magini, M. *Chem. Phys. Lett.* **1979**, *61*, 40−44.
(71) Li, J.; Fisher, C. L.; Chen, J. L.; Bashford, D.; Noodleman, L. *Inorg. Chem.* **1996**, *35*, 4694−4702.
(72) Kallies, B.; Meier, R. *Inorg. Chem.* **2001**, *40*, 3101−3112.
(73) Magini, M. *J. Inorg. Nucl. Chem* **1977**, *39*, 409−412.
(74) Best, S. P.; Forsyth, J. B. *J. Chem. Soc., Dalton Trans.* **1990**, 3507.
(75) Brunschwig, B. S.; Creutz, C.; Macartney, D. H.; Sham, T.-K.; Sutin, N. *Faraday Discuss. Chem. Soc.* **1982**, *74*, 113.

Table 2. Selected Geometrical Parameters for Computed Complexes

complex	pt group	d_{Fe-OH_2} (Å)	d_{Fe-OH}/d_{Fe-O} (Å)	spin multiplicity
$Fe(H_2O)_6^{3+}$	T_h	2.05		6
	$D2h$[a]	2.05		6
$Fe(OH)(H_2O)_5^{2+}$	C_{2v}	2.05	2.05	6
	C_{2v}	2.13[b]	1.76[c]	6
	C_{2v}[a]	2.05	2.05	6
$Fe(OH)_2(H_2O)_4^{+}$ cis	C_s	2.05	2.05	6
$Fe(OH)_2(H_2O)_4^{+}$ cis	C_s	2.235[b]	1.835[b]	6
$Fe(OH)_2(H_2O)_4^{+}$ cis	C_s[a]	2.05	2.05	6
$Fe(OH)_2(H_2O)_4^{+}$ trans	D_{4h}	2.05	2.05	6
$Fe(OH)_2(H_2O)_4^{+}$ trans	D_{4h}	2.18[b]	1.851[c]	6
$Fe(OH)_2(H_2O)_4^{+}$ outer	C_{2v}	2.05	2.05	6
$Fe(OH)_2(H_2O)_4^{+}$ outer	C_{2v}	2.15[b]	1.811[c]	6
$Fe_2(OH)_2(H_2O)_8^{4+}$	D_{2h}	2.05	2.05	5
$Fe_2O(H_2O)_8^{4+}$	D_{2h}	2.05	2.05	5
	D_{2h}	2.05	1.75[d]	5
$Fe_2(H_3O_2)(H_2O)_{10}^{5+}$	C_2	2.05	2.05	5
$Fe_3(OH)_4(H_2O)_{10}^{5+}$	D_{2h}	2.05	2.05	4

[a] Conformations where the planes of the equatorial water molecules are *z*-axis directed. [b] Mean values resulting from computational minimizations.[3] [c] Exact value obtained from calculations.[3] [d] Selected bond length chosen as the half experimental distance between two adjacent ferric ions in polymeric species (~3.5 Å).[73]

previous computed bond lengths[3,68,71] cluster in the upper end of this range from 2.03 to 2.067 Å. On the other hand, some computational studies[3,68] have concluded that in hydroxo complexes the Fe−O(H) bond length is notably shorter than the Fe−O(H_2) one: 1.74−1.851 Å for Fe−O(H) and 2.060−2.296 Å for Fe−O(H_2) considering whole monomeric forms. Therefore, each structure has been computed twice using a constant Fe−O distance whatever the oxygen ligand is and then with two types of Fe−O bond lengths. Finally, the last parameter that needs to be set is the spin multiplicity of each form. Since H_2O and OH^- are weak ligating species according to ligand field theory, all the monomers have 5 single electrons. Previous studies[8] on the magnetic moment of iron(III) aqueous solutions have shown that this property was a function of pH, shifting from ~5.9 μ_B from very acidic media (pH below 0) to ~3.9 μ_B at pH ~ 2.5. Assuming that the formation of oligomeric and polymeric species accounts for this decrease in magnetic moment, 4 single electrons were attributed to the dimers and only 3 to the trimer; this last number is linked to $\mu = 3.9$ μ_B. This magnetic phenomenon in oligomeric species can be due to iron-centered orbitals that overlap or more likely superexchange coupling via the hydroxo (or oxo) bridges.[12] In addition, to check the influence on water molecules arrangements, all the monomers were also built from a D_{2h} symmetry core for $Fe(H_2O)_6^{3+}$, where all the planes of the equatorial water molecules are *z*-axis directed. Major parameters employed to describe the geometry of the computed conformations are presented in Table 2.

Then for each species electronic transitions have been calculated from the difference in energy between molecular orbitals. Two selection rules were applied: the spin multiplicity selection rule ($\Delta S = 0$) and the (Laporte) parity one (the decomposition in terms of single point group of the product between the irreductible representations of the orbitals involved $\Gamma_i \otimes \Gamma_f$ must contain the *x* or *y* or *z* irreductible representation). For each aqua hydroxo complex the results concerning ligand to metal charge-transfer (LMCT) and d−d transitions (when allowed) are presented. No metal to ligand charge transfer was found to be possible above $\lambda = 200$ nm.

In the following discussion some notations will be used to describe the orbitals centered on the ligands. H_2O owns four occupied orbitals. Two orbitals are bonding, one with an axial symmetry that will be called Lσ and a second one with a π symmetry named Lπ; both of them roughly represent O−H bonds using Lewis' formalism. The two electron pairs centered on the oxygen atom that are commonly involved in the Fe−O bond description are nonbonding orbitals nLσ and nLp (σ and p precising the symmetry of the electronic distribution). The term nonbonding indicates that those orbitals are essentially centered on oxygen atoms and therefore do not participate in the description of the usual covalent bonds between O and H in water molecules. For OH^-, one orbital is called Lσ and is linked to the O−H bond; the three others, located on the oxygen, are p-type orbitals nLp. As for the particular ligand $H_3O_2^-$, its diagram consists of 11 molecular orbitals, the last three being empty. The lowest energy one is fully bonding resulting in a σ combination totally in phase noted Lσ^+ and then increasing in energy Lσ^- (with one nodal plane). When one calls *z* the axis directing the O−H−O pattern, *x* the one in the plane of the anion roughly cast on the other O−H bonds' direction, and *y* the one perpendicular to the ion's plane, the other orbitals are Lπ_x^+, Lπ_x^-, nLσ_z^+, nLπ_y^+, nLπ_y^-, and nLσ_z^-. The three antibonding (labeled with *) vacant ones are centered on the bridging hydrogen Lσ_z*, on the single-bond hydrogen atoms Lπ_x*, and one with contributions from every atom with a nodal plane between each atom Lσ*.

$Fe(H_2O)_6^{3+}$. Its diagram of molecular orbitals shows two kinds of allowed transitions from nonbonding p orbitals (nLp) centered on water molecules (T_u symmetry) to d orbitals situated on the ferric ion, the "d_{xy}" type group (T_g) and the "d_{z^2}" one (E_g). Figure 2 presents the comparison between the experimental spectrum and the computed electronic transition wavelengths. To separate and isolate each band, a Gaussian decomposition of the obtained spectrum is proposed. The experimental data feature two major bands centered at $\lambda \sim 190$ and 240 nm. These transitions can be directly linked to the calculations that exhibit two allowed wavelengths at $\lambda \sim 181$ and 229 nm which are related to nLp → $d_{z^2}/d_{x^2-y^2}$ and nLp → $d_{xy}/d_{xz}/d_{yz}$, respectively. So exciting Fe^{3+}_{aq} in the UV region generates the excited species $(Fe^{2+-}H_2O^+)$* via an electronic transfer from nLp orbitals centered on water. Anyway, this means of generation $OH^\bullet$ radicals is only usable in the UV region below 335 nm. In addition considering the weak absorption coefficient of Fe^{3+}_{aq} at the upper range of its electronic spectra plus the fact that the photoreduction quantum yield is pretty low ($\Phi \sim 0.05-0.07$ according to the literature),[28,37,79] this species may not

(76) Herdmann, G. J.; Neilson, G. W. *J. Phys.: Condens. Matter* **1992**, *4*, 627−638.
(77) Kneifel, C. L.; Friedman, H. L.; Newton, M. D. *Z. Naturforsch.* **1989**, *44a*, 385−394.
(78) Ohtaki, H.; Radnal, T. *Chem. Rev.* **1993**, *93*, 1157−1204.

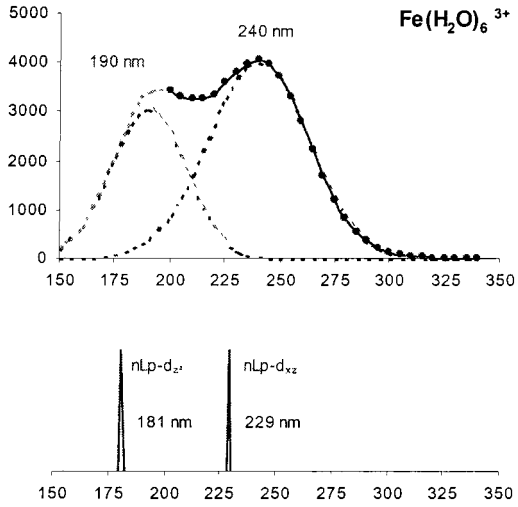

Figure 2. Comparison between the electronic spectrum of $Fe(H_2O)_6^{3+}$ fitted with a Gaussian decomposition (top) and the computed transitions resulting from semiempirical calculations (bottom).

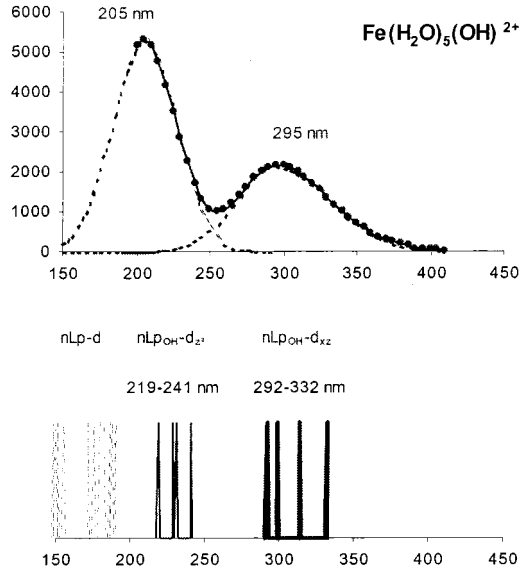

Figure 3. Comparison between the electronic spectra of $Fe(OH)(H_2O)_5^{2+}$ fitted with a Gaussian decomposition (top) and the computed transitions resulting from semiempirical calculations (bottom).

be an important one as regards generation of $OH^{\bullet}$ radicals. Since phototransformation quantum yields generally increase when decreasing excitation wavelengths, one can expect this behavior.[80,81] However, at lowest wavelengths both bands are involved, with different quantum yields of photoreduction probably depending on the antibonding characteristic of the d orbital which electronic density is injected into.

It also has to be noticed that a change in symmetry from T_h to D_{2h} does not notably modify the position in energy of the molecular orbitals and therefore the range of wavelengths involved in the charge-transfer processes, except that with low-symmetry systems the number of allowed transitions increases. However, the set of computed electronic bands is divided into two groups that are pretty narrowly centered at the same locations. This was also checked for the other monomers built from the D_{2h} hexaaqua ion core.

$Fe(OH)(H_2O)_5^{2+}$. Results for the calculated expectable transitions using a constant Fe−O distance of 2.05 Å are shown in Figure 3. There is a good agreement between the two major bands isolated from the decomposition of the experimental spectrum and the charge-transfer computed peaks. The lower energy band centered around $\lambda = 295$ nm can be attributed to an electron transition from nonbonding p orbitals of the OH^- ligand to antibonding "d_{xy}" type ones (estimated to be within the range 292−332 nm). The second one around 205 nm must be a $nLp_{OH} \rightarrow d_{z^2}/d_{x^2-y^2}$ electron transfer even if this second type of transition was calculated to occur for lower wavelengths: from 219 to 241 nm. One could think that part of this second band could be due to nLp → d transfers involving water as an electron donor, but this kind of transition was computed to be situated below 190 nm. Compared to the hexaaquairon(III) ion the shift of the potential photoactivity toward less energy radiations (from 240 to 295 nm) is due to the OH^- ligands that have a HOMO orbital higher in energy than that of H_2O (10.15 eV and up using the same calculation method). Hence transitions from molecular orbitals of the complex centered on the hydroxyl ligand to antibonding metal centered ones require less energy. This $nLp_{OH} \rightarrow$ d LMCT makes this monohydroxo monomer photoactive toward $OH^{\bullet}$ generation up to the visible region and thus can be involved in the hydroxyl radical cycle in natural media (atmospheric droplets or surface water).

In addition, since within the transition state following light excitation $(Fe^{2+}-OH^{\bullet})^*$ the hydroxyl radical is formally formed, then releasing this species may require less structural changes in this case compared to the photoreduction of $Fe(H_2O)_6^{3+}$. That is why one can suggest a higher photolysis quantum yield for hydroxo forms than for Fe^{3+}_{aq}. Lowering the wavelength of excitation here again leads to a shift in the involved transition: from a $nLp_{OH} \rightarrow$ "d_{xy}" to an $nLp_{OH} \rightarrow$ "d_{z^2}" LMCT. Thus, one can expect a slightly change in photoreduction quantum yield while reaching wavelengths close to 200 nm. There are big discrepancies between previous published values of photolysis quantum yield for this species; anyway, for each author we can notice an increase in photoactivity when decreasing excitation wavelength from[28] $\Phi_{360\ nm} = 0.075 \pm 0.008$ to $\Phi_{280\ nm} = 0.287 \pm 0.016$ or from[36] $\Phi_{360\ nm} = 0.017 \pm 0.003$ to $\Phi_{313\ nm} = 0.14 \pm 0.04$. Focusing on the Gaussian decompositon presented in Figure 3, we can see that all these quantum yields have been determined by exciting the same transfer band. Therefore, it is quite consistent that one should get an increase in the rate of generation of $OH^{\bullet}$ radicals while using higher excitation energies, because this enhances the extent of excess energy provided to the excited state. Then according to a recent hypothesis considering that the mechanism of photodissociation of $FeOH^{2+}$ and $FeCl^{2+}$ is a ligand substitution[47] proceeding at the excited-state level, injecting excess energy to vibrating modes involved in the substitution pathway should entail a higher amount of generated hydroxyl

(79) Adamson, M. G.; Baulch, D. L.; Dainton, F. S. *Trans. Faraday. Soc.* **1962**, *58*, 1388−1393.
(80) Zimmermann, G. *J. Phys. Chem.* **1955**, *23*, 825−832.
(81) Adamson, A. W.; Waltz, W. L.; Zinato, E.; Watts, D. W.; Fleischauer, P. D.; Lindholm, R. D. *Chem. Rev.* **1968**, *68*, 541−585.

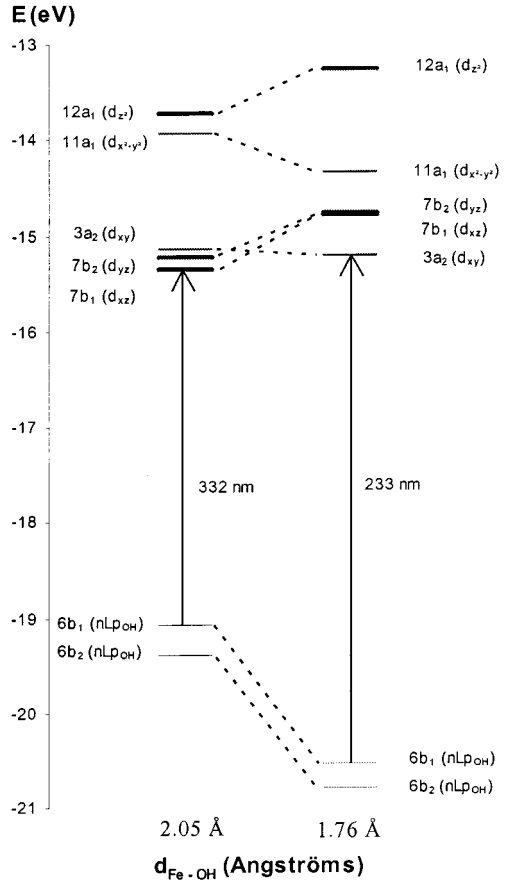

Figure 4. Influence of shortening the Fe−OH bond length in $Fe(OH)^{2+}$, with correlations between the molecular orbitals diagrams. The first authorized electronic transition is mentioned for both geometries from $\lambda =$ 332 nm for $d_{Fe-OH} = 2.05$ Å to $\lambda = 233$ nm for $d_{Fe-OH} = 1.76$ Å.

radicals. This hypothesis is used to interpret the fact that photoreduction quantum yield determinations via laser photolysis experiments can lead to the highest values ($\Phi_{347\ nm} = 0.18-0.24$)[47] compared to more classic works based on steady-state measurements.

About geometrical parameters employed to calculate the molecular orbital diagrams, there is no real incidence in using a D_{2h} basic core instead of an T_h one for $Fe^{3+}{}_{aq}$. On the other hand, using computed shorter bond lengths (1.76 Å) for d_{Fe-OH} notably changes the expectable electronic spectra. Indeed LMCT involving nLp_{OH} type orbitals were then found to be within the range 206−233 nm for the upper one and 165−200 nm for the lower one, which is much different from experimental data. These computed results can be explained by the fact that shortening the Fe−OH distance yields an enhancement of the overlap between the fragment orbitals of these two species. Hence, the bonding molecular orbitals of the complex centered on the hydroxyl group are lowered in energy and symmetrically the energy levels of the antibonding d orbitals located on the metal rise upward. Moreover by emphasis of the interaction along the *z*-axis, all the d orbitals owning a *z* component are rejected higher in energy which modifies the order of the metal-centered orbitals of the "d_{xy}" group. As regards the "d_{z^2}" class, this enlarges the split between its two orbitals. This orbital reorganization is illustrated in Figure 4. Since this calculated

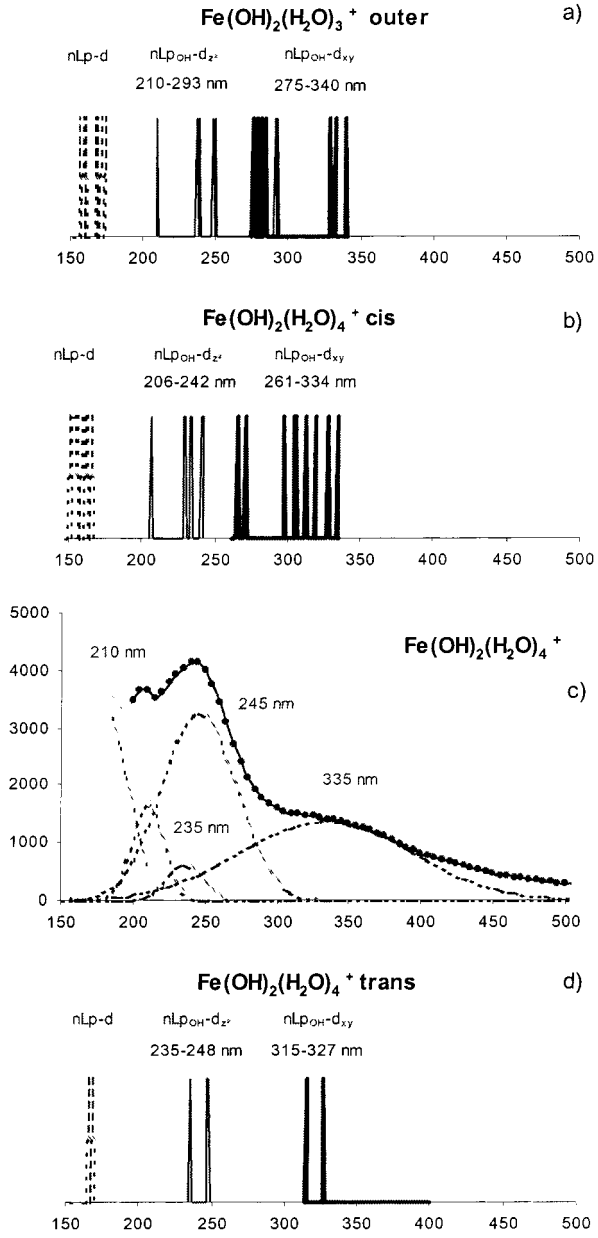

Figure 5. (c) Electronic spectrum of $Fe(OH)_2(H_2O)_4^+$. Computed expectable spectra for the three dihydroxo monomers are presented: (a) the pentacoordinate outer form with two trans hydroxy ligands; (b) the cis isomer; (d) the trans one.

geometry does not account for the experimental spectrum, one can conclude that the computed distance Fe−OH may have been overestimated and may be closer to 2.05 Å than to 1.74−1.76 Å.[3,68] It has to be noted that this last distance is longer than the simple sum of the ionic radii of Fe^{3+} and OH^- considered[70,73] to be about 2.05 Å.

$Fe(OH)_2(H_2O)_4^+$. By maintenance of a constant distance of 2.05 Å for all types of Fe−O bonds, authorized electronic transfers for the three expectable dihydroxo complexes were estimated. The comparison between semiempirical results and the obtained spectrum is given in Figure 5. Each of these three calculations is quite consistent with the experimental data obtained here, which reinforces a posteriori the choice of the panel of aqua hydroxo complex stoichiometries considered and the hydrolysis constants selected as well.

According to recently computed thermodynamics, those species are pretty close in terms of Gibbs free energy,[3] and in the gas phase the cis structure is predicted to be the lowest energy isomer. This thermodynamic preference is reversed in solution, where the trans isomer is predicted to be slightly more stable.[3,82] In both phases the outer pentacoordinated species has an intermediate position in energy. It appeared recently[68] that depending on which basis set is employed for computationnal calculations either pentacoordinate or hexacoordinate form can be predicted as the lowest energy one. However, this new form may only be a mechanism intermediate in the ligand exchange reaction with the solvant, and there is no evidence that this complex can have a long lifetime. Anyway, the fact that these three dihydroxo complexes are close in energy (the difference between ΔG_{298} of the corresponding second hydrolysis was estimated to be about 2 kcal·mol^{-1}) leads us to think that each of them is notably present in solution, at least the classical cis and trans isomers.

The major ligand to metal charge-transfer bands above $\lambda = 200$ nm can be attributed to $nLp_{OH} \rightarrow d$ transitions; for each iron(III) ion, nLp → d transitions involving water are computed to be below 173 nm, which is the weakest energy allowed among all forms. The lowest energy band located at $\lambda \sim 335$ nm is certainly due to a electronic transfer linked to the "d_{xy}" orbital type. As for the 235 and 245 nm peaks revealed by the Gaussian decomposition, they must be $nLp_{OH} \rightarrow d_{z^2}/d_{x^2-y^2}$ bands; in addition their wavelength location well agrees with the calculated results for the trans isomer. Last, the transition isolated for $\lambda = 210$ nm can only be compared to the 206 nm peak (cis species) or the 210 nm one (outer). Thus, this transition can be attributed to the *cis*-dihydroxo form (or the outer pentacoordinated one). Indeed, within this range of wavelengths the potential transitions that could be considered from the high-symmetry trans species are nLp_{OH} (2eg) → d_{z^2} ($5a_{1g}$)/$d_{x^2-y^2}$ ($3b_{1g}$), which are strictly forbidden in terms of parity. However some vibronic coupling may be possible and therefore would allow some electronic promotions in this range. Somehow, through these results, electronic spectroscopy provides us with a sign that the *cis*-$Fe(OH)_2^{+}$ isomer is present in solution even if it is not the more stable one, which is consistent with the fact that these two major structures are really close in energy.

The potential photoactivity of this dihydroxo complex is shifted toward higher wavelengths because of the presence of two high HOMO ligands. In addition, its electronic spectrum has a noticeable extend into solar and visible radiations; thus this iron(III) complex may be involved in photochemical cycling of iron(II/III) in natural media. Since $nLp_{OH} \rightarrow d$ LMCT are responsible for its photon absorbance, $Fe(OH)_2^{+}$ must photochemically lead to OH• radicals generation with a photoreduction quantum yield expected to be roughly close to that of $Fe(OH)^{2+}$. However, this species has not been really studied yet in terms of quantifying its own photolysis rate.

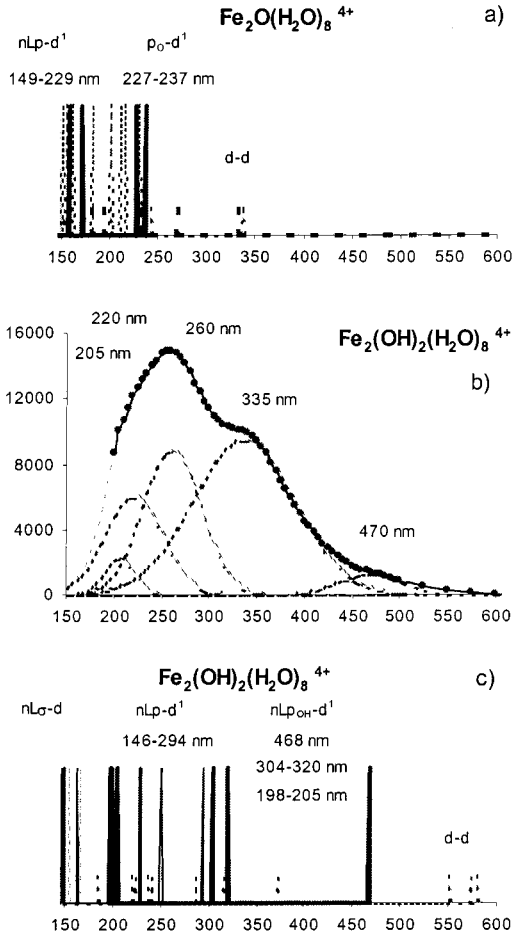

Figure 6. (b) Electronic spectrum of $Fe_2(OH)_2(H_2O)_8^{4+}$. Computed expectable spectra for the two discussed dimers are presented: (a) the dihydroxo form; (c) the μ-oxo one. For each dimer, because of the fact that some d orbitals are full, half-full, or empty ($S = 5$), some d → d transitions are allowed in terms of spin and parity selection rules. They are mentioned as low dashed peaks on the graphs presenting calculated results.

Dihydroxo complexes with short Fe−OH bond lengths (see Table 2) have also been computed. The same kind of observations as that for $Fe(OH)^{2+}$ can be done: shortening the iron−hydroxo distance makes all the electronic transitions move toward higher energy ranges. Particularly $nLp_{OH} \rightarrow d$ transfers are shifted to the zone between 158 and 269 nm for the cis species, 188 and 280 nm for the trans isomer, and 181 and 269 nm for the pentacoordinated one. None of these ranges overlaps significantly the experimental data, particularly considering the tale that goes up to the solar radiation region. Hence here again, one can conclude that the Fe−OH distance of about 1.811−1.851 nm appears to be a bit underestimated and that the real length may be greater. Anyway, there are still some uncertainties concerning the fact that computed model stuctures accurately reflect the iron(III) aqueous species.[68]

$Fe_2(OH)_2(H_2O)_8^{4+}$/$Fe_2O(H_2O)_8^{4+}$. From the results that were found for the monomeric species, a common constant Fe−OH bond length was kept to compute the molecular orbital diagram of the bis(μ-hydroxo) and μ-oxo dimeric forms; their expectable peaks of absorption are compared to the obtained spectra in Figure 6. First of all it has to be mentioned that because of electron pairing d → d transitions

(82) Rustad, J. R.; Felmy, A. R.; Hay, B. P. *Geochim. Cosmochim. Acta* **1996**, *60*, 1553−1562.

can be allowed in terms of the spin selection rule. In addition metal-centered orbitals can be associated due to the dimeric structure and therefore yield to odd symmetry: $5b_{1u}^2$ (d_{yz}), $8b_{2u}^1$ (d_{xy}), $3a_u^1$ (d_{xz}), $7b_{3u}^1$ ($d_{x^2-y^2}$), and $9b_{2u}^0$ (d_{z^2}) for $Fe_2(OH)_2^{4+}$ and $3a_u^2$ (d_{xz}), $6b_{1u}^1$ (d_{yz}), $8b_{2u}^1$ ($d_{x^2-y^2}$), $6b_{3u}^0$ (d_{xy}), and $9b_{2u}^0$ (d_{z^2}) for Fe_2O^{4+}. Hence g → u or u → g internal d−d transitions may occur. However even d−d electron transfers that are authorized in tetrahedral complexes for instance have generally low-intensity absorption coefficients (10^2-10^3 L·mol^{-1}·cm^{-1}).[83] This way even if some of these types of transitions are present among the recorded spectrum, they cannot explain such high values for the extinction coefficient, which is the reason these bands are presented using small peaks in Figure 6. So the discussion will be essentially based on the comparison between the spectrum and the calculated allowed transitions linked to ligand to metal charge transfer. What is obvious is that the results that were obtained using a μ-oxo dimeric structure do not match the experimental curve at all. The highest $p_O \rightarrow d^1$ transition is located at 237 nm, whereas the determined spectrum overlaps largely the visible range up to 470 nm for the last Gaussian band that was extracted from the fit. A second structure has also been roughly checked with shortened Fe−O distances (1.75 Å), but as expected, this yielded to make p_O orbitals sink down to lower energies and then finally gave smaller transition wavelengths. On the other hand, looking at LMCT provided by the calculations for the bis-(μ-hydroxo) form gives really good agreement. The first insight shows that most of the spectrum is due to $nLp_{OH} \rightarrow d^1$ and $nLp(H_2O) \rightarrow d^1$ charge transfers. No transfer up to d^0 orbitals occurs above 200 nm, because the three d^0 empty orbitals are rejected high in energy (there is a ∼2.17 eV split between the last d^1 SOMO and the first d^0 LUMO). The band located at $\lambda = 470$ nm fits with the nLp_{OH} ($5b_{1g}$) → d_{xy}^1 ($8b_{2u}$) transition estimated to be near 468 nm. Then one can attribute the 335 nm shoulder to $nLp_{OH} \rightarrow d_{xz}^1$ ($3a_u$) peaks found to be within the range 304−320 nm, and as regards the shoulders situated around 220 and 260 nm, they must be linked to $nLp(H_2O) \rightarrow d^1$ absorptions calculated for 228 nm (toward $3a_u$) and 250−251 nm (toward $8b_{2u}$). Last, the 205 nm Gaussian curve is probably a set of transitions involving both nLp and nLp_{OH} ligand-centered orbitals. The fact that the computed panel of possible transitions of the Fe_2O^{4+} form does not fit experimental results at all and that there is a good agreement between the calculations made by utilizing the $Fe_2(OH)_2^{4+}$ structure give fairly relevant spectrophotometric clues in favor of the existence of the bis-(μ-hydroxo) dimeric iron(III) ion in aqueous media. Demonstrations of the bis(μ-hydroxo) nature of this dimer were previously brought by utilizing other techniques: magnetic properties studies and infrared spectroscopy.[12,13]

Because of the multiplicity of possible electronic transfers that are involved all along the wavelength range, it is quite difficult to guess what could be the potential photoactivity of this dimer in terms of quantitative tendency. In addition, due to the possible existence of internal d → d transitions,

(83) Huheey, J. E.; Keiter, E. A.; Keiter, L. R. *Inorganic Chemistry*; De Boeck Université: Paris, 1996.

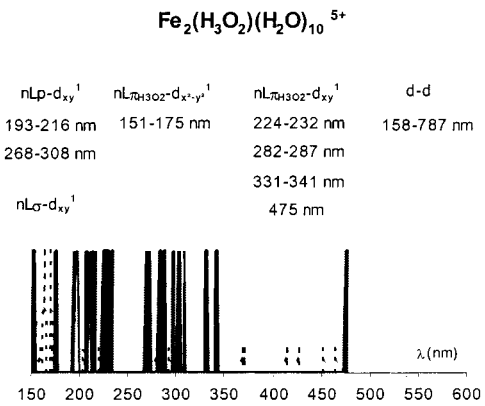

Figure 7. Computed expectable spectra for the hydrogen oxide bridged $Fe_2(H_3O_2)(H_2O)_{10}^{5+}$. Because some d orbitals are full, half-full, or empty ($S = 5$), some d → d transitions are allowed in terms of spin and parity selection rules. They are mentioned as low dashed peaks on the graphs presenting calculated results.

part of the absorbed energy may be utilized for this kind of transfer that will not yield to any release of OH• radicals. This may probably entail a decrease in the amount of really efficient radiations. Below 300 nm nLp → d LMCT involving a water molecule may have reactivity toward OH• formation comparable to that of the iron(III) hexaaqua ion. Considering the $nLp_{OH} \rightarrow$ d charge transfers, since they are linked to bridging ligands, they formally generate a (Fe−μ-OH•−Fe)* excited species, where geminate recombination must be stronger because of the particular location of the hydroxyl radical bond to two iron ions that share a partly reduced degree of oxidation. This nonlability was proposed to account for the poor photoactivity of the dimer;[38] at 350 nm the photolysis quantum yield was found to be ∼0.007.

$Fe_2(H_3O_2)(H_2O)_{10}^{5+}$. Even if this speculated species is assumed to be substantially present only at high concentrations, its charge-transfer spectra have also been computed and are given in Figure 7. Only LMCT transitions from nLp type orbitals are possible above 200 nm. Roughly for each sort of ligand (aqua or hydrogen oxide) electron promotions can be separated into two groups, one tied to transfers toward one high-energy $d_{x^2-y^2}^1$ level and the other one linked to "d_{xy}" type orbitals. All charge transfer are tied to single-occupied d^1 levels. Some d−d transitions are allowed and can be expected over the whole range of wavelengths from UV to near-infrared radiations. Checking MLCT this complex presents no transfer above 156 nm. So from those calculations, one can foresee an electronic spectrum exhibiting five major bands located below 200 nm, at ∼193−232 nm (merged band from two distinct groups of transitions toward "d_{xy}^1" type orbitals), at ∼268−308 nm (merged band here too), at ∼331−341 nm ($nL\pi_{H_3O_2} \rightarrow d_{xy}^1$ electronic promotions), and at ∼475 nm (involving $nL\pi_{H_3O_2}$ electron). It has to be mentionned that the computed spectrum for the hydrogen oxide bridged dimer presented here is close to that of the bis(μ-hydroxo) one, which can mean that, for high ferric concentrations, electronic spectroscopy may not be the more relevant tool for working on the different dimeric species. However, the electronic properties calculated highly depend on the inner O---H---O hydrogen bonds. The value utilized here is given by crystallographic data coming from

Table 3. Labeling of the Spectrophotometric Bands Experimentally Obtained in Terms of Ligand to Metal Charge Transfer

complex	exptl transn bands (nm)	type of charge transfer probably involved	computed location (nm)	calcd highest MLCT wavelength (nm)
$Fe(H_2O)_6^{3+}$	190	$nLp \rightarrow d_{z^2}/d_{x^2-y^2}$	181	132
	240	$nLp \rightarrow d_{xy}/d_{xz}/d_{yz}$	229	
$Fe(OH)(H_2O)_5^{2+}$	205	$nLpOH \rightarrow dz_2/d_{x^2-y^2}$	219−241	148
	295	$nLpOH \rightarrow d_{xy}/d_{xz}/d_{yz}$	292−332	
$Fe(OH)_2(H_2O)_4^{+}$	210	$nLpOH\ (15a') \rightarrow dz^2/d_{x^2-y^2}$ (cis)	206−207	157 (cis)
		$nLpOH\ (5b_1) \rightarrow d_{x^2-y^2}$ (outer)	210	155 (trans)
	235	$nLpOH \rightarrow d_{z^2}/\ d_{x^2-y^2}$	229−248[a]	175 (outer)
	245	$nLpOH \rightarrow d_{z^2}/d_{x^2-y^2}$	229−248[a]	
	335	$nLpOH \rightarrow d_{xy}/d_{xz}/d_{yz}$	261−334[a]	
$Fe_2(OH)_2(H_2O)_8^{4+}$	205	$nLp(H_2O) \rightarrow d_{xz}^1\ (3a_u)/(4b_{2g})$	196−204	170
		$nLpOH \rightarrow d_{x^2-y^2}^1\ (7b_{3u})$	198−205	
	220	$nLp(H_2O) \rightarrow d_{xz}^1\ (3a_u)$	228	
	260	$nLp(H_2O) \rightarrow d_{xy}^1\ (8b_{2u})$	250−251	
	335	$nLpOH \rightarrow d_{xz}^1\ (3a_u)$	304−320	
	470	$nLpOH\ (5b_{1g}) \rightarrow d_{xy}^1\ (8b_{2u})$	468	

[a] Calculated wavelength range considering the common cis and trans isomers.

well-defined compounds[59,66,67] that have been synthesized and then characterized, which is not the case of the aqueous iron(III) one. So one can conclude that the $d_{O-O} = 2.5$ Å length must be in the upper part of the range of conceivable O−H−O distances. Elongating the hydrogen bonds' length would lessen the strength of the H bonds present in this dimer, which could be therefore intuitively broken down into two separated fragments linked via a H bridge, $[Fe^{III}(H_2O)_5\text{-}HO\text{---}H^{+}\text{---}OHFe^{III}(H_2O)_5]^{5+}$. Thus, putting forward the hypothesis that the hydrogen bond slightly disrupts the two monomeric patterns, the spectroscopic properties of this extended dimer would be roughly built from those of $Fe(OH)^{2+}$. This would yield a totally different expected computed spectrum, which was checked using a H bond length of $d_{O-H} = 1.75$ Å, from which no LMCT band occur above $\lambda \sim 300$ nm.

As regards the photoactivity of this dimeric form, the more accessible charge transfers involve $nL\pi_y^{+}/nL\pi_y^{-}/nL\sigma_z^{-} \rightarrow d^1$ transitions that strip one electron from an orbital centered on the oxygen atoms, formally giving HO---H---OH•, which is a potential source of OH• radicals. However, the fact that each formal OH^{-} is double-linked to Fe^{III} and to H^{+} can entail a quite small photoreduction quantum yield by promoting back-recombinations instead of radical releasing. So, the photoactivity of this species might be much smaller than that of the $Fe(OH)^{2+}$ fragments it could be made from.

$Fe_3(OH)_4(H_2O)_{10}^{5+}$. To get some insights into the photochemical behavior of the trimeric form, its possible charge-transfer peaks were estimated in Figure 8. Here some internal $d \rightarrow d$ transitions are also allowed by parity rules because of couplings of orbitals centered on several ferric ions. As for LMCT, they are essentially linked to $nLp_{OH} \rightarrow d^1$ and $nLp(H_2O) \rightarrow d^1$ transitions. Nonoccupied d^0 orbitals are here again strongly rejected toward high energy; the gap between the last occupied level $6b_{2u}^1$ (d_{yz}) and the first empty one $8b_{1g}^0$ ($d_{x^2-y^2}$) is about 5.84 eV. Therefore, no electron can be promoted toward d^0 orbitals from the ligands utilizing radiation above 200 nm. What has to be noticed is that this species exhibits a large involvement with the visible region through several expected absorbances ($nLp_{OH} \rightarrow d^1$) situated around ∼350, ∼450, ∼550, and ∼650 nm. This can explain the darkness of high-concentration aqueous solutions of iron(III) salts containing oligomeric and polymeric species on the basis of the structure of the trimer that is presently computed. Multiplying the number of transitions up to the near infrared accounts for a steady constant absorption all along the range of visible wavelengths. Numerous bands appear to be able to occur between 200 and 300 nm; so one can expect a large charge-transfer zone divided into multiple shoulders finally yielding a huge band of absorption centered around 240 nm. Anyway, no metal to ligand charge transfer is expected above 128 nm according to the molecular orbital diagram.

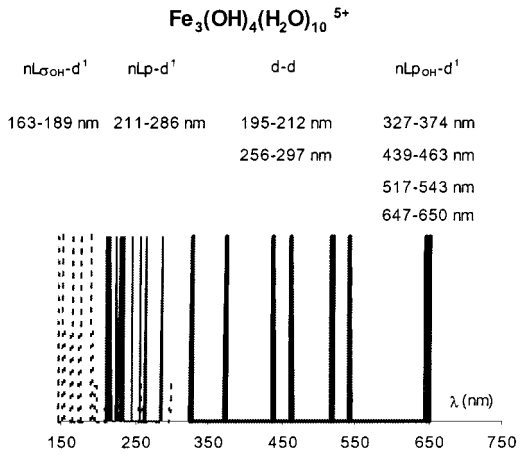

Figure 8. Estimated peak locations for $Fe_3(OH)_4^{5+}$ trimer. Some $d \rightarrow d$ transitions are allowed in terms of spin and parity selection rules; they are mentioned as low dashed peaks.

Conclusion. Recently $Fe(H_2O)_6^{3+}$ was found to be the best π-acceptor in terms of bond orbital analyses among the 3d hexaaqua ions.[72] Therefore, since π overlap between the orbitals of the metal and the water molecules tends to enhance the antibonding characteristic of the d molecular orbitals, one can expect that injecting electronic density up to this kind of antibonding level should lead to the breaking of the metal−ligand bond. This can explain why iron(III) aqua hydroxo complexes are such good candidates for OH• radical generation following a ligand to metal charge-transfer excitation. Table 3 sums up the set of bands extracted from the spectra of each species; computed limits for MLCT are also given, but they are certainly not involved within the

observed transitions. However, the photoreduction quantum yields must depend on the type of ligand the electron is promoted from and on structural characteristics such as the particular location of the hydroxyl anions in the oligomeric species.

It has to be mentioned that works on iron(III) aqueous hydrolysis products strongly depend on the validity of the thermodynamic constants utilized for reaching speciations. The considered species and equilibrium constants used in this work were selected and discussed from reviews. No sign for any form other than the (1,0), (1,1), (1,2), and (2,2) stoichiometries was noticed through extrapolations from experimental data. Furthermore, the fact that computed band locations match well-determined spectra seems to indicate a posteriori that the set of selected hydrolysis constants correctly describes the iron(III) distribution. Such a work finally provided a large study of the most common iron(III) aqueous species from an electronic spectroscopy point of view, and their potential activities have been reached through the molar coefficients determined here and the labeling of the observed bands.

Acknowledgment. We thank Prof. Michel Pélissier (University of Poitiers) for having provided us with the Hyperchem software package, and we also thank the peer reviewers for the helpful comments they made.

Supporting Information Available: Listings of calculated molecular orbitals energies for every aqua hydroxo complex's computed structure. This material is available free of charge via the Internet at http://pubs.acs.org.

IC011029M